

Dynamic resonant matching method for a wireless power transmission receiver

Eberhard Waffenschmidt, Senior Member IEEE,
Cologne University of Applied Science,
Betzdorferstraße 2, D-50679 Cologne, Germany
eberhard.waffenschmidt@fh-koeln.de

This paper is a contribution to the **Special Issue on Wireless Power Transfer, 2015**

Keywords: Wireless power transmission, resonant matching

Abstract — Wireless power transmission systems can be optimized by matching the resonance frequency of a receiver. However, in certain applications, such as e.g. a multi-receiver system, it is desired to match the individual resonance frequencies of the receiver to a fixed (e.g. common) operation frequency.

In this publication, a method is proposed to match the resonant frequency dynamically without changing the physical value of the components. Instead, it is changed “virtually” by a method, which is named “frozen resonance state” by the author. The basic idea is to maintain the state of a resonant circuit (to “freeze” the state) for a fraction of the resonant period, e.g. by freewheeling the current of the resonant inductor or maintaining the voltage of the resonant capacitor. This additional time extends virtually the resonant period leading to an effective lower resonant frequency. By adjusting the additional time, the effective resonant frequency can be matched to the operation frequency individually for each receiver.

This publication explains the basic idea more in detail and gives an overview of the different possible circuit topologies. Furthermore, the method is applied to an exemplary receiver of a capacitive wireless power transmission system, where measurements are presented.

I. INTRODUCTION

Wireless power transmission and especially inductive wireless power transmission is a hot topic in the field of power electronics, as numerous recent publications show. Since Nicola Tesla’s time one century ago it is obvious that operating in resonance improves the power transfer system [1][2][3][4][5]. As pointed out in [4] and [5], operating in resonance may either optimize the transfer efficiency or the received power. To optimize power efficiency, not only operating in resonance, but also suitable load matching is necessary. Then, efficiencies of more than 90% can be achieved, if the distance of the transmitter coil and the receiver coil is not larger than their diameter [3].

However, the resonance frequency, which allows maximized power transfer, is dependent on the magnetic coupling factor between the coils [5]. Also the optimal load matching is a function of the coupling factor [3]. In most real life wireless power system, the coupling factor is not well determined because of position or components variations [6][7]. To overcome problems with varying coupling factor, some proposals exist to limit its variation. In reference [8] a winding design for planar coils is derived to achieve a position independent coupling factor as long as transmitter coil and receiver coil overlap. Reference [9] gives an overview of further approaches to achieve an independency of the position.

These approaches do not cover component variations. To control an output parameter in the receiver, e.g. the output voltage, a straight forward approach is to apply a DC-to-DC converter in the receiver. Different possible principles for

such applications are described in reference [10]. However, a DC-to-DC converter cannot change the receiver’s resonant frequency in order to maximize power transfer. Therefore, wireless power transmission systems are proposed, which adapt the operating frequency to the resonance frequency of the receiver [11].

For single receiver systems this is a suitable approach, but not for systems with multiple receivers [12][13][14][15][16][17][18]. Then, special care must be taken to match the resonance frequencies to control the power flow. In addition, cross coupling effects between the receivers may appear [12][15]. To overcome such effects and to control the power flow, reference [16] proposes to use different resonant frequencies in the receivers and to operate the transmitter alternatively on the different resonance frequencies. Based on a similar principle, reference [17] proposes to use switchable filters in the receivers in order to match them to different frequencies. And reference [18] proposes a time sharing technique serving the different resonant receivers one after the other.

But all these technologies require some kind of feedback and power transmission is always a compromise between the different receivers. Matching the receivers to a single operating frequency of the transmitter gives a larger flexibility and a simpler system design. This requires modifying the resonant circuit in the receiver. One known method is to add or remove switchable capacitors to the resonant circuit in the receiver [19][20][21][22]. This way, not only the resonance frequency, but also the load impedance can be matched to the optimal operation point [19]. Such capacitor banks allow only discrete values. In

addition, this requires an additional power switch for each of the capacitors. Therefore, they may be combined with Varactors to achieve a non-discrete control [20][21]. But they are available only for small capacity values and are therefore suitable only for solutions in the higher MHz range. Another possibility is to switch dynamically between two differently matched states to control the output voltage in a kind of pulse width modulation scheme [22].

A variation of the resonance frequency can also be achieved with a variable inductor. Reference [11] proposes a saturable inductor to match a transmitter. In reference [23] such a device is used to dynamically match the receiver's resonant circuit. This way a continuous control of the resonance frequency is possible. But especially for small receivers such additional components are bulky and disadvantageous.

As a further approach, the inductivity of the resonant inductor is virtually varied without changing its physical value [24][25][26]. This is achieved by switching the current through the inductor dynamically. The basic idea is to modify the inductor current with the same inductor voltage, which leads to a variation of the effective inductivity. This is called a "phase-controlled variable inductor" [24], "switched inductor" [25], or "dynamically switched inductor" [26]. In references [24] and [25] the inductivity of the main resonant circuit is varied, and in reference [26] an additional inductor parallel to the resonant circuit varies the resonant frequency.

In this publication, this idea is generalized and a method is proposed to match the resonance frequency of a receiver dynamically without changing the physical value of the resonant components. Instead, the resonance frequency is changed "virtually" by a method, which is named "frozen resonance state" by the author. Only one switch is required, which, however, needs to be fast switching. The method allows a continuous control instead of discrete steps. The method primarily results in a controlled reduction of the resonance frequency from the natural resonance frequency. Therefore the natural resonance frequency must be selected as upper limit.

First, the principle is explained and related equations are derived. Then the theory is validated with circuit simulations of simple arrangements. Further possible topologies are explained then. Finally, the method is applied to an exemplary receiver of a capacitive wireless power transmission system, where measurements are presented in order to demonstrate the proposed principle.

II. THE "FROZEN RESONANCE STATE" PRINCIPLE

A. Basic idea

The basic idea is explained with the help of a mechanical analogon of a resonant device. Imagine a pendulum or a children's swing, which is hold fixed for a while every time it reaches its outer position, e.g. by a mechanical break or simply by holding the swing. During the time, the swing is hold, the energy state of the swing is preserved. When it is

released, the swing swings just as normal again in a resonant cycle. Now, imagine an excitation of the swing, which has a lower frequency than the resonant frequency of the swing. When you hold the swing for a short amount of time, you can match the swing frequency to the excitation frequency and optimize the driving force of the excitation. This basic idea is to maintain the state of a resonant circuit (to "freeze" the state) for a fraction of the resonant period. Therefore, the method is named "frozen resonance state" by the author.

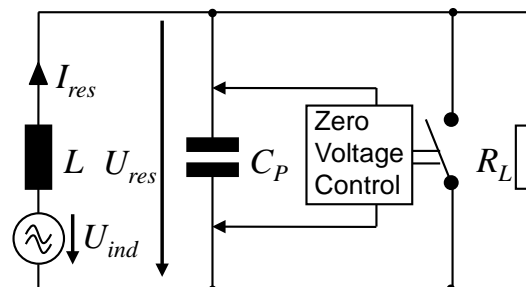


Figure 1: Parallel resonant inductive power receiver with "frozen resonance state" circuit.

A similar action can be achieved in an electrical resonant circuit, e.g. by letting the current of the resonant inductor freewheel or maintaining the voltage of the resonant capacitor. This additional period of time extends virtually the resonant period leading to an effective lower resonant frequency. By adjusting the additional period of time, the effective resonant frequency can be matched to the operation frequency. It is obvious that this way the effective resonance frequency can only be lowered. When the method is applied, one has to select the natural resonance frequency as upper limit of the frequency range.

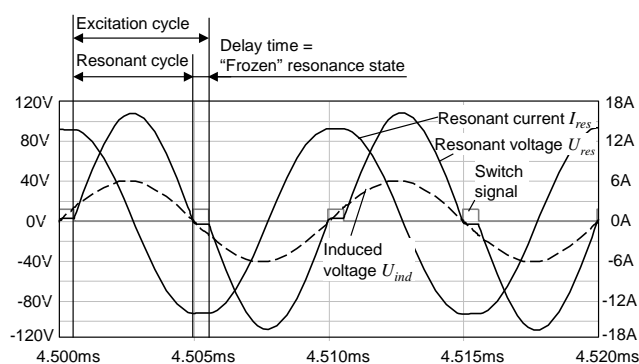


Figure 2: Resonant voltage and current, generator voltage and switch control voltage.

A circuit, which can do such an action, is illustrated in Figure 1. It might relate to an inductive wireless power receiver consisting of a receiver coil L with a parallel resonant capacitor C_P . Figure 2 shows the time dependence of related voltages and currents (voltage and current values are not related to Figure 1 and for illustration only). In the coil, a voltage U_{ind} is induced, which can be considered as

the sinusoidal excitation with an operation frequency f_{op} . In parallel to the resonant circuit, a switch may short circuit the capacitor and allow the resonant inductor current I_{res} to freewheel through the switch. The switch is closed every time, when the resonant voltage across the capacitor U_{res} becomes zero. By letting the inductor current I_{res} freewheel, the energy state of the resonant circuit is preserved until the switch is opened again. Figure 2 shows that during this time the resonant current I_{res} is maintained constant, and the resonant voltage U_{res} is maintained zero (of course, since the switch is closed). It also shows that the extension of the resonant cycle matches the excitation cycle, such that the circuit now operates in resonance.

The principle of preserving the energy of a resonant circuit for a certain time appears in some applications previously described in literature. As one example, extended period quasi-resonant DC-to-DC converters make use of something close to it [27][29][28]. This has been shown for a down converter [27] and a boost converter [28]. An overview of different applications is given in [29]. Basically, in such a circuit the resonance cycle is split into two parts, each of them relating to the switching action of the main circuit. In between, the energy is preserved to be used for the next switching action.

A similar idea leads to resonant gate drivers [30][31][32][33][34]. Here, it becomes more obvious that the desired wave shape is close to a square wave function and only the transitions relate to a resonant behaviour. The main switching action is attributed to a part of a resonant cycle. In between the switching action the energy is preserved or re-used in one or the other way. In [30] and [31] the gate capacitor remains at its charging state and thus preserves the resonant state. This is similar to the principle in this paper. In [33] the energy is recovered to the supply capacitor using diodes and [34] uses a similar principle with active switches. Here, the energy is no longer saved in the resonant circuit itself, but externally. This is different from the application in this paper.

In all these cases the preservation of the resonant energy is meant neither to modify a resonant frequency nor to match the circuit to a periodical excitation.

B. Calculation theory

To calculate the behaviour, one has to consider that the circuit is non-linear. It is possible to investigate the circuit either in the time domain or in the frequency domain.

First, the view on the frequency domain is explained: If the switch is closed shortly after a positive zero voltage crossing, a short positive current pulse is generated in the switch, in parallel to the capacitor. The fundamental frequency of this pulse has a phase shift of nearly -90° with respect to the voltage. This corresponds to an additional capacitive current, which is added to the resonant circuit. Then, the switch can be considered as a virtual capacitor. It reduces the resonance frequency. The length of the pulse determines the amplitude of the current and thus the value of

the virtual capacitor. By varying the length of the pulse, the value can be adjusted such that the resulting resonance frequency matches the operating frequency. In order to calculate the change of resonance frequency, a Fourier analysis would be necessary, and the fundamental frequency would need to be considered. This approach is not further derived and is mentioned just for broadening the understanding of the circuit.

In the time domain, the general idea has been explained already. To calculate the time behaviour, related differential equations apply. However, there are two cases: When the switch is open, and when the switch is closed. During the time period when the switch is open, the circuit behaves like a normal resonant circuit. When the switch is closed, the state of the circuit is preserved and thus everything is simply delayed in the time domain. Concluding, the circuit behaves like a conventional resonance circuit, which is excited with a signal, which has period being reduced by the delay time(s) t_d . From this consideration, an equivalent operation frequency f_{equ} can be derived from the real operation frequency f_{op} :

$$f_{equ} = \frac{1}{\frac{1}{f_{op}} - 2 \cdot t_d} \quad (1)$$

To make it symmetrical, a delay t_d is introduced twice in a period, every time when the voltage crosses zero. This results in factor 2 in the equation.

This equivalent frequency f_{equ} can now be used to calculate currents and voltages for an arbitrary operation frequency f_{op} . The quality factor and the characteristic impedance of the equivalent resonance circuit relate to a resonant circuit running at its natural resonance frequency determined by the values of the inductor L and capacitor C. No further equations are necessary.

C. Validation of the theory by simulations

To validate the theory, a time domain simulation was done with LT-SPICE by Linear Technology. Figure 3 shows the used circuit diagram. The topology is similar to the one in Figure 1. The resonant circuit consists of an inductor $L_{res} = 10 \mu\text{H}$ and a capacitor $C_{res} = 180\text{nF}$. The natural resonance frequency of this resonant circuit is $f_{res} = 118.6 \text{ kHz}$. This doesn't match the operation frequency of $f_{op} = 100 \text{ kHz}$ provided by the generator source $V_{gen} = 10 \text{ V}$. To detect the zero voltage crossing, two switches S3 and S4 are used as comparators, one for the positive and one for the negative edge. Capacitor C3 and R3 generate pulses from the output signal of the comparators. They are compared to a pulse control voltage provided by source B1 using switches S3 and S5. Their output is a pulse, where its length depends on the pulse control voltage. The dependence of the pulse length on the control voltage is non-linear and shown in Figure 4, including a fit function. The two pulses (one for the positive and one for the negative

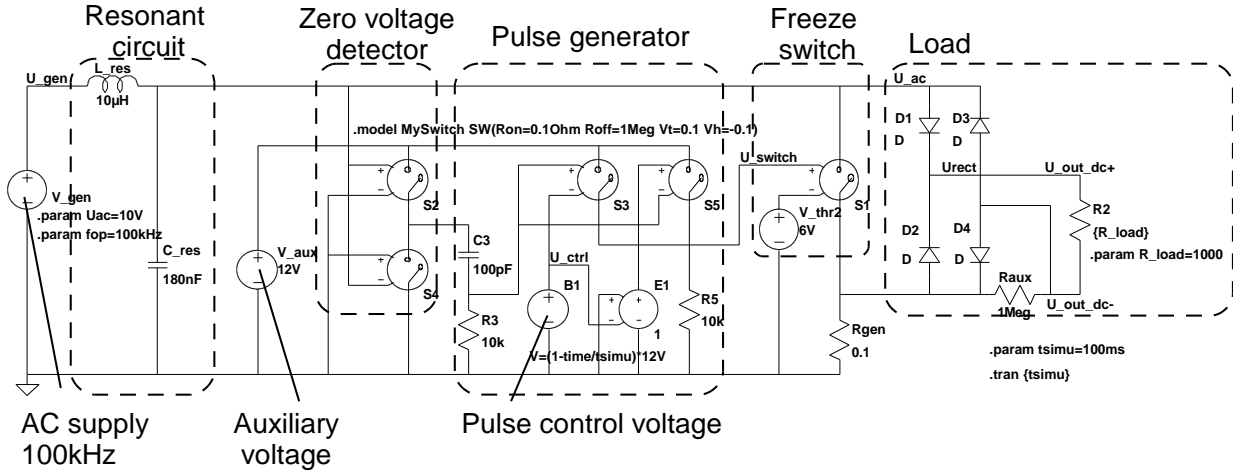


Figure 3: Circuit diagram for the LT-SPICE simulation.

slope) are added to control the freeze switch S1, which shorts the resonant circuit. The load consists of a bridge rectifier and the load resistance R_{load} . An auxiliary resistor R_{aux} is added to achieve stable simulation runs.

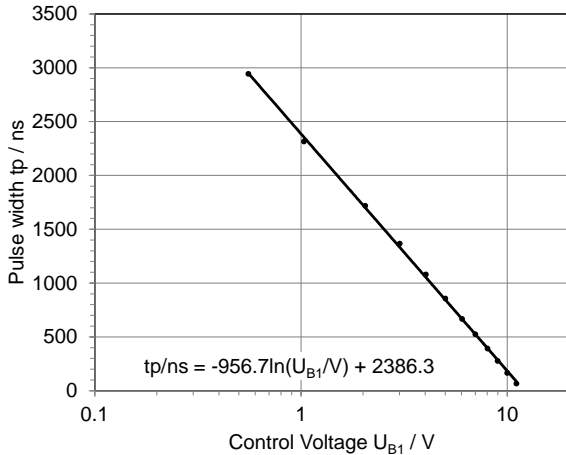


Figure 4: Pulse width as function of the pulse control voltage in the simulation circuit.

During one simulation run the pulse control voltage is linearly reduced from 12 V to 0 V over the time. This way, the pulse time is increased over the simulation time from a 0 to approximately 3 μ s.

Simulations are done with three different load resistors $R_{load} = 1 \text{ k}\Omega$, 100Ω and 10Ω . Figure 5 shows the resulting output voltage. The pulse width increases with the simulation time. It is shown as additional horizontal axis. The gray filled areas relate to the LT-Spice simulations. Clearly, a resonance peak is visible at a pulse length of $t_d = 8 \mu$ s. Applying equation (1) with $f_{op} = 100 \text{ kHz}$ results $f_{equ} = 119.05 \text{ kHz}$ as equivalent resonance frequency. This matches very well the natural resonance frequency of $f_{res} = 118.6 \text{ kHz}$.

The three graphs show different resonance peaks for the three load resistance. Quality factors $Q = 49.5$, 11.2 and 1.2 for the load resistances of $R_{load} = 1 \text{ k}\Omega$, 100Ω and 10Ω can be derived from the figures.

According to the assumptions of the previous chapter, a characteristic impedance $Z_C = (L_{res}/C_{res})^{0.5} = 7.45 \Omega$ can be derived. However, this would result in somewhat lower load resistances. Probably, losses in the rectifier diodes account for these additional losses in the simulation. An additional parallel resistance of $R_P = 500 \Omega$ would match these losses.

To further validate the assumptions of using an equivalent frequency, the output voltage U_{out} is calculated by a simple impedance model. It results from a complex voltage divider according to the following equation:

$$U_{out} = V_{gen} \cdot \frac{R \parallel \left(\frac{1}{j \cdot 2 \cdot \pi \cdot f_{equ} \cdot C_{res}} \right)}{j \cdot 2 \cdot \pi \cdot f_{equ} \cdot L_{res} + R \parallel \left(\frac{1}{j \cdot 2 \cdot \pi \cdot f_{equ} \cdot C_{res}} \right)} \quad (2)$$

where R is the load resistance R_{load} in parallel with R_P . An additional small parasitic capacitor accounting for diode capacities could be added in parallel to R_P to get even closer to reality.

The equivalent frequency is calculated according to equation (1) using the related pulse width. From the pulse width the simulation time t_{sim} is calculated using Figure 4 to match the results to the time domain simulations. The results are compared to the time domain simulations in Figure 5. A reasonable match also left and right from the resonance peak can be observed. Only for $R_{load} = 10 \Omega$ a larger deviation is visible. Using equation (2) leads to a shift of the resonance frequency to below 100 kHz because of the topology, which cannot be observed in the case of the frozen resonance state

circuit. Maybe, the additional losses considered with R_P should be considered differently. However, it can be concluded that the simulations prove the calculation concept of the frozen resonance state principle.

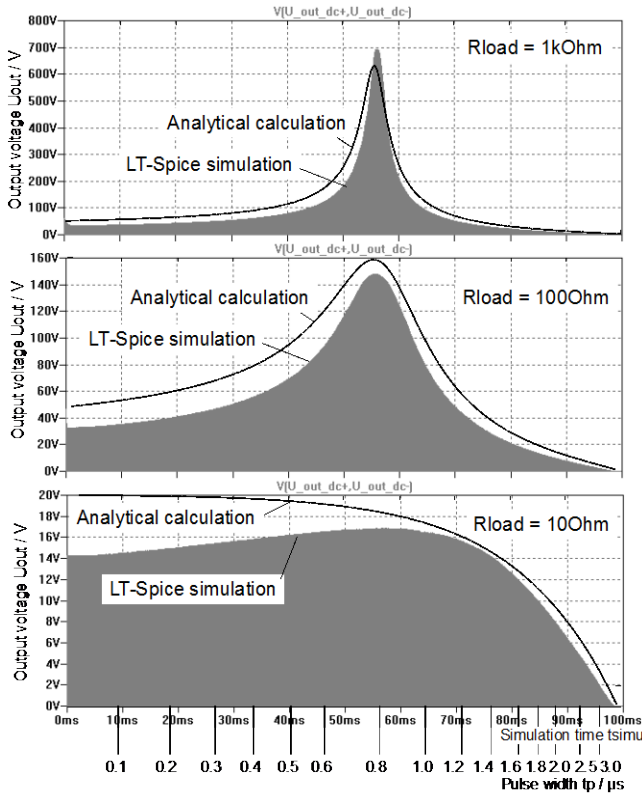


Figure 5: Simulation results for the output voltage compared to analytical calculations.

III. DIFFERENT TOPOLOGIES

In principle, the resonance state may be “frozen” at any time. However, using a switch implies limits. Since on a switch either the current is zero or the voltage is zero, only those resonance states may be frozen, which relate to zero current or zero voltage. This requires either a zero voltage control (ZVC) or a zero current control (ZIC). One can sort the different possible topologies according to this property.

A. Zero voltage control topologies

The first topology in the previous chapter was a ZVC topology. For an inductive wireless power receiver, further ZVC topologies are possible, which can make use of the frozen resonance state principle. Figure 6a, b and c show such arrangements.

To consider their functionality, it is best to analyze the situation in the frequency domain, similar as explained in the previous chapter. As explained, the frozen resonance state pulse can be considered as an additional virtual capacitor. So, here one can check, what effect an additional capacitor at the place of the switch would have.

In Figure 6a, this additional capacitor would be placed directly in parallel to the existing capacitor and thus has a simple, direct and significant effect.

In Figure 6b, the original circuit is a series resonant circuit. The additional virtual capacitor adds a parallel capacitor to the receiver coil. Here, the effect is not straight forward. The resonance frequency will also reduce, but the combination of parallel and series capacitor will also change the matching of the load resistance to the generator voltage.

Figure 6c has a similar effect. Also here, the series resonant circuit is extended by a virtual parallel capacitor. It also affects the matching of the load to the generator voltage.

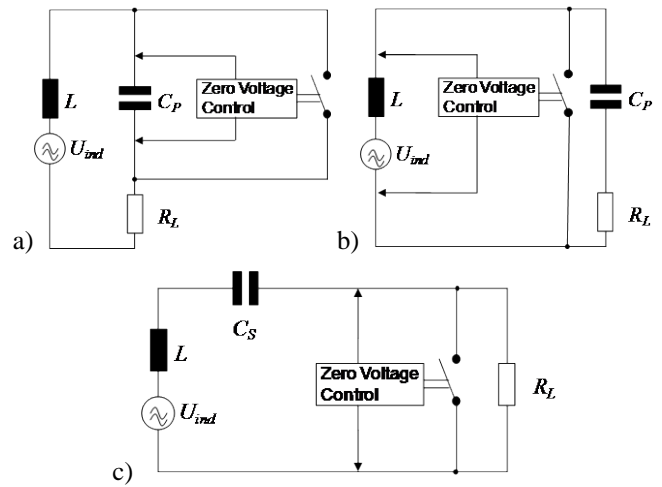


Figure 6: ZVC switch in parallel to a) the resonant capacitor, b) receiver inductor, c) the load.

B. Zero current control topologies

By placing the freeze switch in series of the resonant circuit, ZIC topologies are possible. In these topologies the switch is normally closed and only during the freeze time it is open. As a disadvantage, such topologies have higher losses, because of the on-resistance of the switch.

A ZIC switch generally adds a voltage pulse in series to the circuit. With considerations similar to those in chapter II, such a pulse can be considered as the influence of a virtual inductor placed in series. This also lowers the resonance frequency. Taking this into account, the different topologies shown in Figure 7a, b and c can be evaluated.

Figure 7a shows ZIC switch in series to the series capacitor. This arrangement adds a series virtual inductor to the series resonant circuit and is thus straight forward. The behaviour can easily be described with the previous equations.

Figure 7b adds a virtual inductor in series to the parallel resonant capacitor. Then, the resulting circuit becomes a mixture of a series and parallel resonant circuit. The resonance frequency will reduce, but also the matching of the load will change.

In Figure 7c, a virtual inductor is added in series to the resonant inductor of the parallel resonant circuit. Here, the

virtual inductor simply adds to the real one making the case straight forward to analyse.

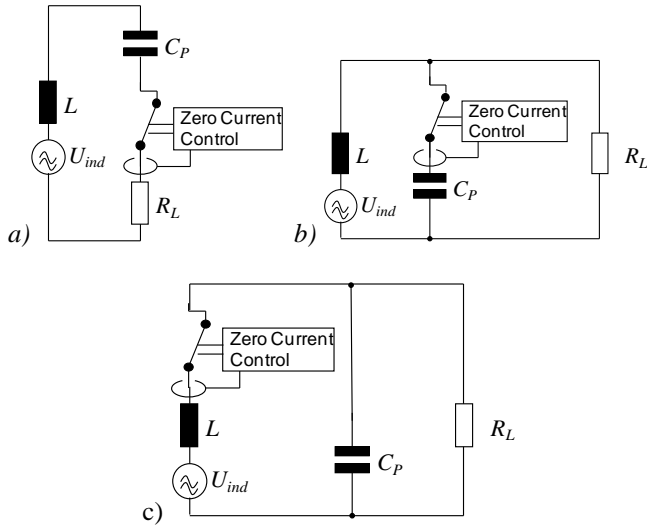


Figure 7: ZIC switch in series to the a) series capacitor, b) parallel capacitor, c) receiver coil.

C. Capacitive receiver topologies

A similar approach can be used in capacitive wireless power receivers. In such a receiver, the resonant capacitor is split into two capacitors. The capacitor electrodes are made from copper plates. One electrode of these capacitors belongs to the transmitter and the other to the receiver. Figure 8 illustrates the arrangement. An inductor in the receiver can match the receiver as resonant circuit to the operating frequency.

Figure 8 illustrates two examples of a ZIC and a ZVC arrangement. A further topology is presented in the following chapter as demonstrator.

The ZIC switch (Figure 8a) simply adds an additional virtual inductivity and thus influences the resonance frequency straight forward according to equation (1).

In Figure 8b the switch adds a virtual capacity in parallel to the resonant inductor. This also lowers the resonance frequency. But it also changes the matching of the load.

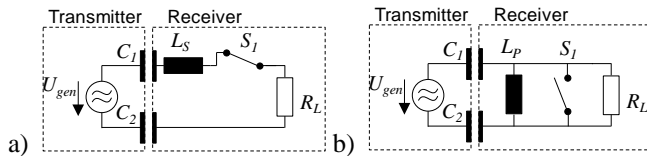


Figure 8: Arrangements for capacitive receiver with a ZIC switch (a) and with a ZVC (V) switch.

IV. DEMONSTRATOR

A demonstrator circuit is designed and fabricated. It relates to a capacitive wireless power receiver as illustrated in Figure 9. The resonant capacitors consist of copper plates, one half in the receiver and the other half in the transmitter. The resonant inductor is used to match the

receiver and improve the power transmission. Here, a ZVC structure parallel to the inductor is used. It is quite similar to the topology in chapter II.B, because here also the current freewheels during the frozen state. Figure 11 and Figure 12 show the related realization of the circuit diagram. Figure 10 shows a photograph of the circuit in operation.

Figure 11 shows the power part and relates more or less to Figure 9. The freeze switch is realized with two anti-serial connected MOSFETs. The load is a series connection of 10 power LEDs.

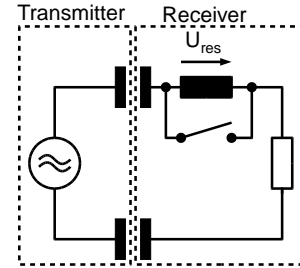


Figure 9: Principle arrangement of the demonstrator.

Figure 12 shows the control circuit. Its structure is similar to the simulation circuit in Figure 3. The controlled switches are replaced by fast comparators. C_{10} and C_{11} compensate for the delay of the comparators and must carefully be selected by hand. The comparators also have an external hysteresis (R_5 , R_8) to allow for stable operation. The control circuit is operated with a 9 V block battery.

The pulse width is set manually by the potentiometer R_{20} setting the pulse control voltage. This demonstrator is intended to demonstrate the basic functionality of the frozen resonance principle. The manual adjustment allows measurements with stable pulse widths.

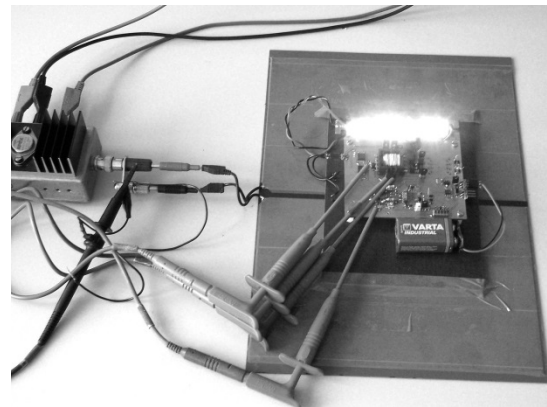


Figure 10: Photograph of the demonstrator circuit in operation.

In a later step (not presented in this paper) a feedback loop can be introduced to control the length of the pulse according to the output voltage or any other parameter. The control of the output voltage is not straight forward. The pulse length must be set in such a way that the virtual

resonance frequency is always higher or always lower than the operating frequency. Then, a monotone rising or falling dependence of the output voltage on the pulse width can be achieved.

In order to account for device tolerances, a smart control is recommended, which is able to detect the case, when this dependence changes from monotone rising to falling. A control can also be used to maximize the power reception. Then the control can be based on a maximum power point (MPP) algorithm. Reference [23] gives a good overview of the control of such a system.

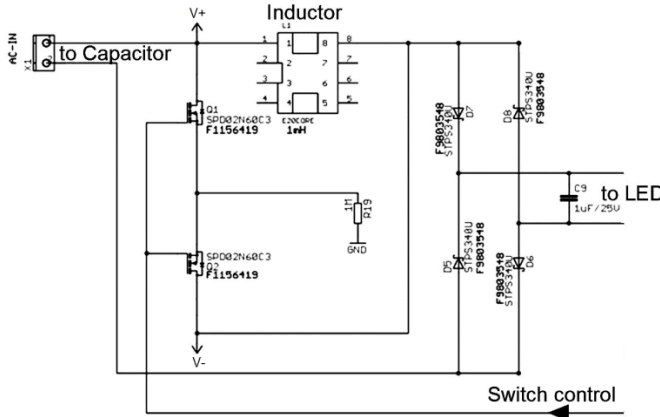


Figure 11: Circuit diagram of the power part.

The circuit is operated with a power amplifier providing the generator voltage. Figure 13 shows measured voltage and current curves in three different operation points. Similar to Figure 2 the figure shows the generator voltage (Channel 3), which is pretty sinusoidal. Channel 2 shows the freeze switch signal. The different pulse widths are clearly visible. The channel 1 shows the voltage across the resonant inductor. Clearly visible is that an optimal pulse width exists (figure b). If the pulse width is small (figure a), the inductor

voltage is low. This corresponds also nearly to the case, where no frozen resonance state principle is used. If the pulse width is too large (figure c), the inductor voltage decreases again. Here, the equivalent operating frequency exceeds the resonance frequency and thus no matching is obtained.

V. CONCLUSION

Concluding, a method is proposed to match the resonant frequency of a receiver dynamically without changing the physical value of the resonant components. Instead, the resonant frequency is changed “virtually” by a method, which is named “frozen resonance state” by the author. The basic idea is to maintain the state of a resonant circuit (to “freeze” the state) for a fraction of the resonant period, e.g. by letting the current of the resonant inductor freewheel or maintaining the voltage of the resonant capacitor. This additional period of time extends virtually the resonant period leading to an effective lower resonant frequency. By adjusting the additional period of time, the effective resonant frequency can be matched to the operation frequency individually for each receiver.

A simple calculation method in the frequency domain has been proposed, which makes use of an equivalent operating frequency, which can easily be calculated from the width of the “freeze” pulse. This method has successfully been validated by time domain simulations. Furthermore, the general principle has been proven by measurements on a demonstrator circuit.

ACKNOWLEDGMENT

Thanks to my former colleagues at Philips Research, who supported this work. I’d especially like to mention the colleagues in the electronic workshop for the manufacturing of the related hardware.

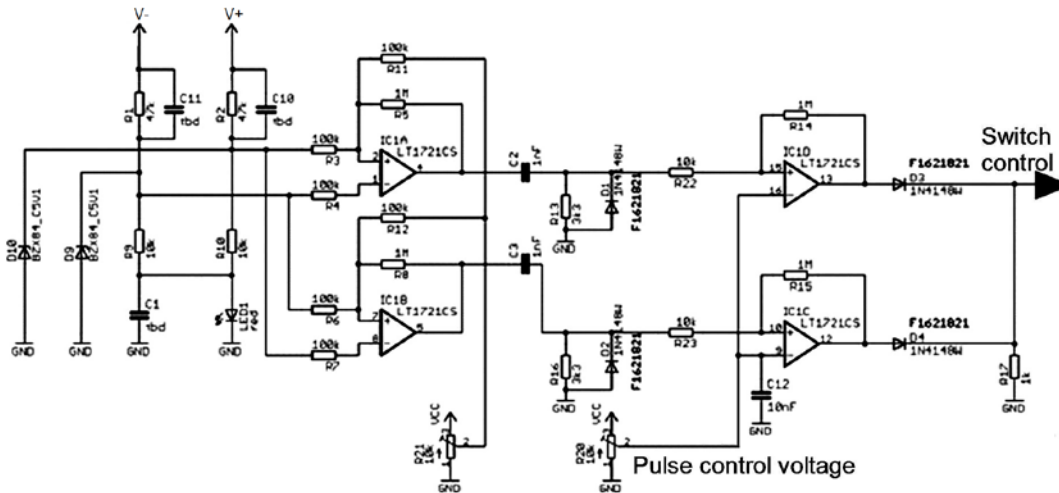
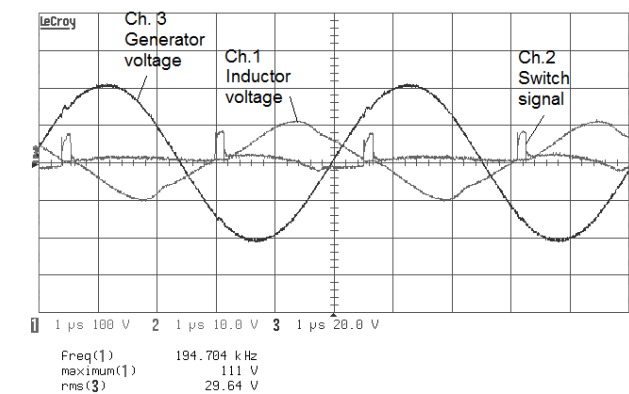
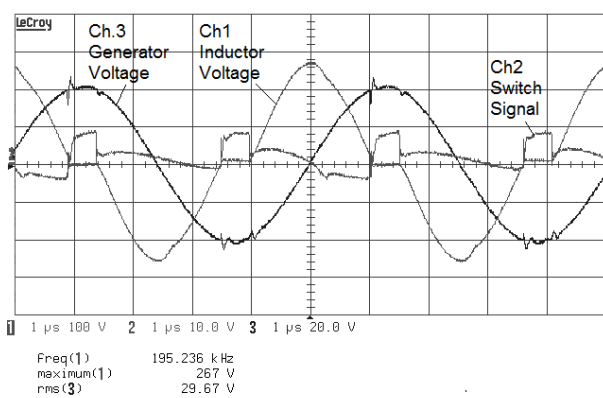


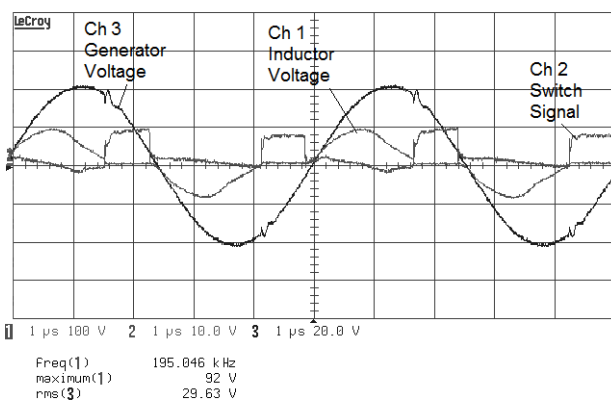
Figure 12: Circuit diagram of the pulse generator



a)



b)



c)

Figure 13: Oscilloscope screenshots of different pulse widths: a) Pulse width too small. b) Pulse width matches resonance. c) Pulse width too long.

REFERENCES

[1] M. Pinuela, D. C. Yates, S. Lucyszyn, P. D. Mitcheson, "Maximizing DC-to-Load Efficiency for Inductive Power Transfer", IEEE Transactions on Power Electronics, Vol. 28, No. 5, May 2013, pp.2437-2447.

[2] W. Zhang, S.-Ch. Wong, Ch. K. Tse, Q. Chen, "Analysis and Comparison of Secondary Series- and Parallel-Compensated Inductive Power Transfer Systems Operating for Optimal Efficiency and Load-Independent Voltage-Transfer Ratio", IEEE Transactions on Power Electronics, Vol.29, No. 6, June 2014, pp.2979-2990.

[3] E. Waffenschmidt, T. Staring, "Limitation of Inductive Power Transfer for Consumer Applications", 13th European Conference on Power Electronics and Applications (EPE 2009), Barcelona, Spain, 8.-10.Sept. 2009, paper #0607.

[4] S. Y. R. Hui, W. Zhong, C. K. Lee, "A Critical Review of Recent Progress in Mid-Range Wireless Power Transfer," IEEE Transactions on Power Electronics, Vol. 29, No. 9, Sep. 2014, pp. 4512-4520.

[5] E. Waffenschmidt, "Wireless Power for Mobile Devices", Proceedings of the 33rd International Telecommunications Energy Conference (INTELC 2011), Amsterdam, The Netherlands, 9.-13. Oct. 2011.

[6] S. Raju, R. Wu, M. Chan, C. P. Yue, "Modeling of Mutual Coupling Between Planar Inductors in Wireless Power Applications", IEEE Transactions on Power Electronics, Vol. 29, No. 1, Jan. 2014, pp.481-490.

[7] Y. Su, X. Liu, S. Y. R. Hui, "Mutual Inductance Calculation of Movable Planar Coils on Parallel Surfaces", 39th Power Electronic Specialists Conference (PESC) 2008, Rhodes, Greece, 15. - 19. June 2008, p.3475,

[8] E. Waffenschmidt, "Free Positioning for Inductive Wireless Power System", IEEE Energy Conversion Congress & Exposition (ECCE 2011), Phoenix, Arizona, USA, 17.-22.Sept. 2011.

[9] J. P. C. Smeets, T. T. Overboom, J. W. Jansen, E. A. Lomonova, "Comparison of Position-Independent Contactless Energy Transfer Systems," IEEE Transactions on Power Electronics, Vol.28, No.4, April 2013, pp.2059-2067.

[10] J. T. Boys, G. A. Covic, A. W. Green, "Stability and Control of Inductively Coupled Power Transfer Systems", IEE Proceedings Electric Power Applications, Vol. 147, No. 1, Jan 2000, pp. 37-43.

[11] S. Aldhafer, P. C.-K. Luk, J. F. Whidborne, "Electronic Tuning of Misaligned Coils in Wireless Power Transfer Systems," IEEE Transactions on Power Electronics, Vol.29, No.11, Nov. 2014, pp. 5975-5982.

[12] Z. Pantic, K. Lee, S. Lukic, "Receivers for Multi-Frequency Wireless Power Transfer: Design for Minimum Interference", accepted for publication in a future issue of IEEE Journal of Emerging and Selected Topics in Power Electronics (online Dec. 2014).

[13] K. K. Ean, B. Teck Chuan, T. Imura, Y. Hori, "Novel Band-Pass Filter Model for Multi-Receiver Wireless

- Power Transfer via Magnetic Resonance Coupling and Power Division”, Proceedings of the 13th IEEE Annual Wireless and Microwave Technology Conference (WAMICON), 15.-17. April 2012.
- [14] J. Kim, H.-C. Son, D.-H. Kim, Y.-J. Park, “Impedance Matching Considering Cross Coupling for Wireless Power Transfer to Multiple Receivers”, Proceedings of the 2013 IEEE Wireless Power Transfer (WPT) Conference, Perugia, Italy, 15. – 16. May 2013.
- [15] D. Ahn, S. Hong, “Effect of Coupling Between Multiple Transmitters or Multiple Receivers on Wireless Power Transfer”, IEEE Transactions on Industrial Electronics, Vol. 60, No. 7, July 2013, pp. 2602-2613.
- [16] Y. Zhang, T. Lu, Z. Zhao, F. He, K. Chen, L. Yuan, “Selective Wireless Power Transfer to Multiple Loads Using Receivers of Different Resonant Frequencies”, accepted for publication in a future issue of IEEE Transactions on Power Electronics (online Dec. 2014).
- [17] W. Zhong, S.Y.R Hui, “Auxiliary Circuits for Power Flow Control in Multi-Frequency Wireless Power Transfer Systems with Multiple Receivers”, accepted for publication in a future issue of IEEE Transactions on Power Electronics (online Dec. 2014).
- [18] J. Park, S. Nam, “Analysis of Wireless Power Transfer Characteristics for Multiple Receivers by Time Sharing Technique”, Journal of the Korean Institute of Electromagnetic Engineering and Science, Vol. 11, No. 3, Sept. 2011, pp. 183-185
- [19] Y. Lim, H. Tang, S. Lim, J. Park, “An Adaptive Impedance-Matching Network Based on a Novel Capacitor Matrix for Wireless Power Transfer,” IEEE Transactions on Power Electronics, Vol.29, No.8, Aug. 2014, pp. 4403-4413.
- [20] S. S. Toncich, E. T. Ozaki, A. H. Mohammadian, “Method and Apparatus for Adaptive Tuning of Wireless Power Transfer”, US Patent Application, US 20090284220 A1, Priority date 13. May 2008.
- [21] Y.-K. Jung, B. Lee, “Design of Adaptive Optimal Load Circuit for Maximum Wireless Power Transfer Efficiency”, Proceedings of the 2013 IEEE Asia-Pacific Microwave Conference (APMC), pp. 1221 – 1223.
- [22] P. Si, A.P. Hu, S. Malpas, D. Budgett, "Switching Frequency Analysis of Dynamically Detuned ICPT Power Pick-ups", Proceedings of the 2006 International Conference on Power System Technology (PowerCon 2006), 22.-26. Oct. 2006, pp.1-8.
- [23] M. Zaheer, N. Patel, A. P. Hu, “Parallel Tuned Contactless Power Pickup Using Saturable Core Reactor”, Proceedings of the 2010 IEEE International Conference on Sustainable Energy Technologies (ICSET), 6.-9. Dec. 2010, Kandy, Sri Lanka, pp. 1 – 6.
- [24] A. P. Hu, S. Hussmann, "Improved Power Flow Control for Contactless Moving Sensor Applications," IEEE Power Electronics Letters, Vol.2, No.4, Dec. 2004, pp. 135- 138.
- [25] J. James, J. Boys, G. Covic, "A Variable Inductor Based Tuning Method for ICPT Pickups," Proceedings of the 7th International Power Engineering Conference (IPEC 2005), Vol. 2, 29.Nov.-2.Dec. 2005, pp.1142-1146.
- [26] M. Yang , X. Li, Z. Ao , Y. Wang, „Transferred Power Control for ICPT Pick-ups Utilizing Dynamically Switched Inductor”, Proceedings of the 2012 International Conference on Future Energy, Environment, and Materials, Energy Procedia 16, 2012, pp. 1440 – 1447.
- [27] I. Barbi, J.C.O. Bolacell, D.C. Martins, F.B. Libano, "Buck Quasi-Resonant Converter Operating at Constant Frequency: Analysis, Design, and Experimentation", IEEE Transactions on Power Electronics. Vol. 5. No. 3. July 1990, pp. 276-283.
- [28] S. Y. R. Hui, K. W. E. Cheng, S. R. N. Prakash, "A Fully Soft-Switched Extended-Period Quasi-Resonant Power-Factor-Correction Circuit", IEEE Transactions on Power Electronics, Vol. 12, No. 5, Sept. 1997, pp.922-930
- [29] K. W. E. Cheng, P. D. Evans “A Family of Extended-Period Circuits for Power Supply Applications Using High Conversion Frequencies”, 4th European Conference on Power Electronics and Applications 1991 (EPE’91), Firenze, Italy, 3.-6. Sept. 1991, pp. 4.225–4.230.
- [30] H. Fujita, “A Resonant Gate-Drive Circuit With Optically Isolated Control Signal and Power Supply for Fast-Switching and High-Voltage Power Semiconductor Devices”, IEEE Transactions on Power Electronics, Vol.28, No.11, Nov. 2013, pp. 5423-5430.
- [31] R. Chen, F.Z. Peng, “A High-Performance Resonant Gate-Drive Circuit for MOSFETs and IGBTs,” IEEE Transactions on Power Electronics, Vol.29, No.8, Aug. 2014, pp. 4366-4373.
- [32] D. M. van de Sype, A. P. M. van den Bossche, J. Maes, J. A. Melkebeek, “Gate-Drive Circuit for Zero-Voltage-Switching Half- and Full-Bridge Converters”, IEEE Transactions on Industry Applications, Vol. 38, No. 5, Sept./Oct. 2002, pp 1380 – 1388.
- [33] Y. Chen, F. C. Lee, L. Amoroso, Ho-Pu Wu, “A Resonant MOSFET Gate Driver With Efficient Energy Recovery”, IEEE Transactions On Power Electronics, Vol. 19, No. 2, March 2004, pp. 470 – 477.
- [34] W. Eberle, Y.-F. Liu, P.C. Sen, “A New Resonant Gate-Drive Circuit with Efficient Energy Recovery and Low Conduction Loss”, IEEE Transactions on Industrial Electronics, Vol. 55, No. 5, May 2008, pp. 2213 – 2221.